

Electronic and optical properties of antiferromagnetic iron doped NiO – A first principles study

John E. Petersen,¹ Fidele Twagirayezu,¹ Luisa M. Scolfaro,¹
Pablo D. Borges,² and Wilhelmus J. Geerts¹

¹Department of Physics, Texas State University, San Marcos, Texas 78666, USA

²Instituto de Ciências Exatas e Tecnologia, Universidade Federal de Viçosa,
38810-000 Rio Paranaíba, MG, Brazil

(Presented 3 November 2016; received 23 September 2016; accepted 7 November 2016;
published online 6 February 2017)

Antiferromagnetic NiO is a candidate for next generation high-speed and scaled RRAM devices. Here, electronic and optical properties of antiferromagnetic NiO: Fe 25% in the rock salt structure are studied and compared to intrinsic NiO. From density of states and complex dielectric function analysis, the first optical transition is found to be at lower frequency than intrinsic NiO due to an Fe impurity level being the valence band maximum. The resulting effects on refractive index, reflectivity, absorption, optical conductivity and loss function for Fe-doped NiO are compared to those of intrinsic NiO, and notable differences are analyzed. The electronic component of the static dielectric constant of NiO: Fe 25% is calculated to be about 2% less than that of intrinsic NiO. © 2017 Author(s). All article content, except where otherwise noted, is licensed under a Creative Commons Attribution (CC BY) license (<http://creativecommons.org/licenses/by/4.0/>). [<http://dx.doi.org/10.1063/1.4975493>]

I. INTRODUCTION

Interest in antiferromagnetic NiO has increased recently due to its potential application in radiation hard, low energy, and high speed resistive RAM (RRAM) devices. The switching mechanism is based on reversible soft dielectric breakdown, where an applied electric field causes diffusion of O vacancies through nanofilaments, resulting in the change from a high to a low resistance state.¹⁻⁴ Bulk NiO has an indirect optical band gap of approximately 4.0 eV.⁵⁻⁷ Traditional Density Functional Theory (DFT) studies underestimate this value, yet limitations of the local density approximation (LDA) can be overcome by methods which correct for correlation of d levels, such as using the HSE06 functional, the GW method, or including a Hubbard potential U. Calculations including a Hubbard potential, adding an on-site Coulomb interaction, have been shown to be accurately descriptive of the underlying physics of NiO.^{1,3,6-8} Thus, we use this computationally inexpensive method to study the electronic and optical properties herein.

While NiO has been studied extensively, little work has been done with antiferromagnetic NiO: Fe.¹⁻¹⁷ Most experimental works studying NiO: Fe focus on its magnetic properties for applications in spintronics devices. These studies use solution-based preparation of nanoparticles, in oxygen-rich conditions, resulting in formation of Fe₂O₃ and NiFe₂O₄ crystallites for Fe concentrations in ferromagnetic NiO: Fe between 2-5%.^{5,15,18-21} The high surface to volume ratio of the nanoparticles results in interesting ferromagnetic properties.²² With sputter deposition – a type of physical vapor deposition – oxygen levels can be finely tuned to achieve near-stoichiometric or oxygen-poor antiferromagnetic NiO: Fe, for application in RRAM devices. The phase diagram of the Ni-Fe-O system reports a stable rock salt structure for iron concentrations up to 40 at.% in a low oxygen atmosphere.²³ Reports of others on dual ion beam sputtered NiO: Fe (19 at. % Fe) and RF magnetron sputtered NiO: Fe confirm the rock salt crystal structure for films sputtered at low oxygen pressure.^{24,25} At lower concentrations, Yan, et al. have found a NaCl rock salt phase for pulsed laser deposition grown Ni_{0.98}Fe_{0.02}O, as well.²⁶ Our DFT study on NiO: Fe with oxygen vacancies is forthcoming; however, here, we study the system with a stoichiometric concentration of oxygen.



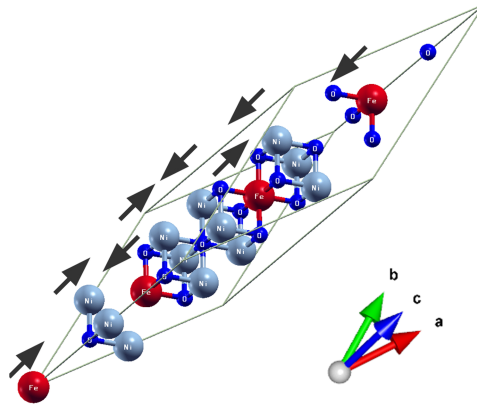


FIG. 1. 32 atom supercell of NiO: Fe 25%. Adjacent metal (111) planes are antiferromagnetically aligned, as the arrows indicate.

We show results for the band structure and density of states, along with imaginary and real parts of the complex dielectric function calculated from eigenvalues of said band structure and a Kramers-Kronig transformation, respectively, as done in our previous work on NiO.¹ Effects – of doping NiO with a high concentration of Fe – on the refractive index, reflectivity, absorption, optical conductivity, and loss function are analyzed, and compared to those of pristine NiO. We have calculated electronic and optical properties of 6.25%, 12.5%, and 25% antiferromagnetic Fe-doped NiO, and found 25% Fe to be representative of the range of concentrations. For the sake of brevity, only this concentration will be discussed here.

II. COMPUTATIONAL DETAILS

Calculations in this work were performed within DFT using the Vienna ab Initio Simulation Package (VASP) and the projector augmented wave (PAW) method, using the Generalized Gradient Approximation (GGA) of Perdew, Berke, and Ernzerhoff (PBE) for exchange and correlation.^{27–29} A Hubbard potential U (DFT+ U) was included to account for correlation of valence d shell electrons, as is customary for calculations of transition metal oxides.³⁰ It has been shown that this method is more than sufficient to describe physical properties of NiO.^{1,3,6,31} A value of 5.3eV was used for the effective Hubbard potential for both Ni and Fe. A collinear spin-polarized approach was used in all calculations. A 32-atom rhombohedral supercell, keeping the antiferromagnetic ordering of NiO along the [111] direction, was used (Figure 1), with a $4 \times 4 \times 4$ k-point grid and a 520 eV energy cutoff. Fe concentration was considered at 25%, positioned symmetrically to maintain the antiferromagnetic order. We have found alternative arrangements increase energy by as much as 300 meV for the 12.5% case and are often ferromagnetic. All calculations were performed at $T = 0$ K with fully relaxed cells, minimizing the forces on the ions to less than 0.02 eV/angstrom. From the band structures, optical properties were calculated within the independent particle approximation, neglecting local field effects.³²

III. RESULTS AND DISCUSSION

The octahedral coordination causes crystal field splitting in the d shells of the transition metal ions. In intrinsic NiO, the valence band maximum is comprised of a mixture of Ni e_g and fully occupied t_{2g} , while the conduction band minimum is comprised of Ni e_g .^{1,6} In Figure 2, we show the band structure and the local density of states (LDOS) for NiO: Fe. When 25% of Ni atoms are replaced by Fe atoms in NiO, and since Fe has two electrons less than Ni, the t_{2g} level of Fe is pushed up to the Fermi Energy, becoming the highest fully occupied state, and the conduction band minimum remains Ni e_g . This result is in agreement with the experimental work of Yan, et al.²⁶ The magnitude of the magnetization of Ni and Fe sites is found to be 1.70 and

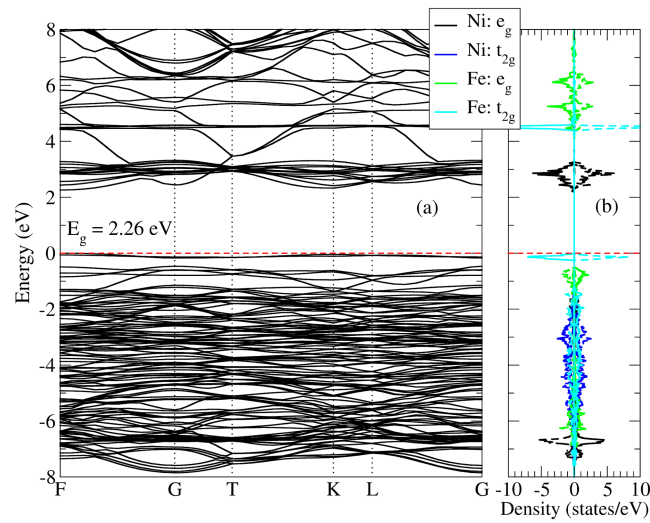


FIG. 2. Band Structure along the high symmetry lines in the Brillouin zone (a) and Local Density of States (LDOS) (b) for the majority and minority spins for the NiO: Fe system. The localized t_{2g} level of Fe is below the Fermi energy (red dashed line) and reduces the band gap. The conduction band minimum is comprised of Ni e_g . In the LDOS plot, two Ni and two Fe atoms are chosen from planes with antiferromagnetic alignment. Dashed lines are from the metal ion's counterpart in an opposite magnetically polarized plane.

3.75 Bohr magnetons, respectively, with the antiferromagnetically aligned magnetizations summing to a net magnetic moment of zero at the ground state. Previous theoretical works using GGA + U have found Ni to have a magnetization of 1.67 in intrinsic NiO.³¹ The introduction of the t_{2g} level of Fe reduces the calculated band gap from intrinsic NiO by about 1.0 eV, from 3.29 to

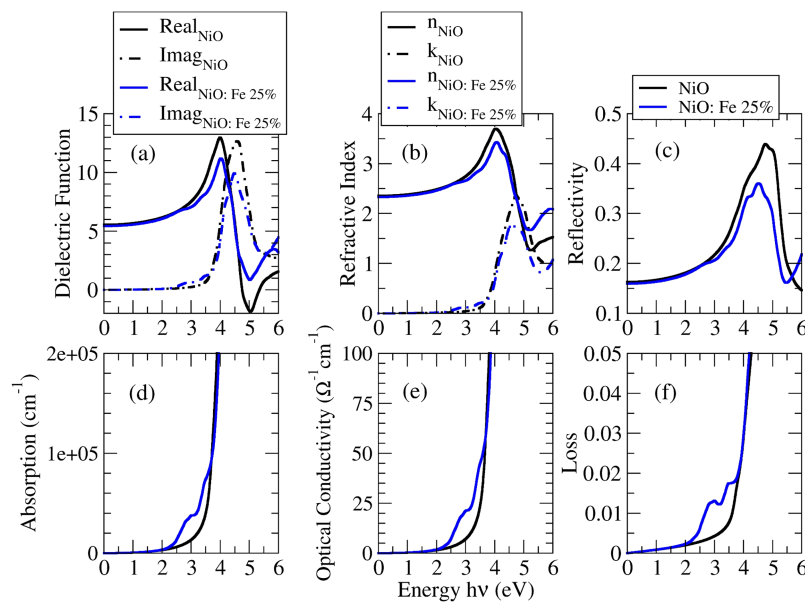


FIG. 3. Calculated optical properties comparing intrinsic NiO with NiO: Fe 25%. The low frequency dielectric function (a) and complex refractive index (b) change little with the addition of Fe. However, notable differences can be seen at higher frequency. Reflectivity (c) is reduced substantially at high frequency with introduction of Fe. Absorption (d), optical conductivity (e), and loss (f) show an increase right at the energy corresponding to the band gap of NiO: Fe 25% that is not present for intrinsic NiO. NiO: Fe 25% is about a third less lossy (f) than intrinsic NiO at high frequency (not shown in scale).

2.26 eV. This reduction in the band gap from the t_{2g} level of Fe has a direct effect on the optical properties.

In Figure 3, we show the calculated optical properties for the xx component of the frequency dependent dielectric tensor, along with properties derived from these values of NiO and NiO: Fe. Our results for intrinsic NiO agree very well with available experimental data.^{16,17,33} The calculated value of 5.54 for the optical component of the real static dielectric function is close to that of the experimental value reported to be 5.7.³³ The calculated refractive index of 2.35 matches that of the experimental value of 2.33.⁴ Furthermore, calculated optical conductivity agrees well with recent experimental results.¹⁷

For NiO: Fe, refractive index, extinction coefficient (Fig 3(b)), and absorption (Fig 3(d)), are in line with previously published ellipsometry data.⁹ The reduced band gap seen for Fe-doped NiO is reflected in the imaginary component of the dielectric function: due to the reduced energy necessary to promote an electron to the conduction band, the first optical transition can be seen to occur at lower frequency than in intrinsic NiO. This can be seen further in the derived absorption and optical conductivity (Figures 3(d) and 3(e), respectively): due to the reduced band gap, absorption is found at lower frequency in NiO: Fe than the intrinsic case. Doping with Fe decreases the reflectivity and loss function at high frequency, yet loss increases around 2 eV (Figures 3(c) and 3(f), respectively), which is at much higher energy than peak operating frequency of RRAM. Adding Fe to NiO is found to reduce the electronic dielectric constant by 0.12, even though FeO has a dielectric constant about twice that of NiO (9.24-11.13).³⁴ This may indicate that the addition of Fe affects the diffusion of oxygen in the filaments.³⁵ These results can help to guide experimental characterization of antiferromagnetic Fe-doped NiO for use in RRAM devices.

IV. SUMMARY AND FINAL REMARKS

Optical and electronic properties of NiO: Fe 25% were calculated and compared to that of intrinsic NiO. The values calculated for intrinsic NiO agree well with the experimental and theoretical data in the literature. Optical properties of rock salt antiferromagnetic NiO: Fe have not been studied extensively, and theoretical results are seen here for the first time. From a LDOS calculation of $\text{Fe}_{0.25}\text{Ni}_{0.75}\text{O}$, we have shown the character of the valence band maximum to differ from that of intrinsic NiO. The ground state converges to Fe t_{2g} being the highest fully occupied state, rather than Ni e_g or t_{2g} . Consequently, the calculated band gap is reduced, and the independent particle approximation reveals the first optical transition to be at slightly lower frequency than intrinsic NiO. However, it should be noted that an additional optical transition was not found, indicating the material behaves more like an alloy than a doped system, with the Fe t_{2g} level taking on the role of the Ni t_{2g} level in intrinsic NiO. The calculated electronic component of the real static dielectric function of NiO: Fe, at zero frequency, was found to be about two percent less than the calculated value of intrinsic NiO. The effects on refractive index, reflectivity, absorption, optical conductivity and loss function are evidently caused by the first optical transition being at a slightly lower energy than intrinsic NiO. These calculated values can assist in experimental characterization via optical methods. Future work will study the stoichiometry of the filaments, including cases with varying oxygen vacancy concentration, which we predict will result in additional induced states in the band gap with notable effects on optical properties.

ACKNOWLEDGMENTS

Financial support from DOD (HBCU/MI grant W911NF-15-1-0394) is acknowledged. LS also thanks support from the Materials Science, Engineering, and Commercialization program of Texas State University.

¹ J. Petersen, F. Twagirayezu, P. D. Borges, L. Scolfaro, and W. Geerts, *MRS Adv.*, [First View Online](#) (2016).

² J. Dawson, Y. Guo, and J. Robertson, *Appl. Phys. Lett.* **107**, 122110 (2015).

³ B. Magyari-Köpe, S. Park, H. Lee, and Y. Nishi, *J Mater. Sci.* **47**, 7498 (2012).

⁴ R. Powell and W. Spicer, *Phys. Rev. B* **2**, 2182 (1970).

⁵ Y. Lin, J. Wang, J. Cai, M. Ying, R. Zhao, M. Li, and C. Nan, *Phys. Rev. B* **73**, 193308 (2006).

⁶ C. Rödl, F. Fuchs, J. Furthmüller, and F. Bechstedt, *Phys. Rev. B* **79**, 235114 (2009).

- ⁷ R. Gillen and J. Robertson, *J. Phys.: Condens. Matter* **25**, 165502 (2013).
- ⁸ F. Tran, P. Blaha, and K. Schwarz, *Phys. Rev. B* **74**, 155108 (2006).
- ⁹ M. S. Compton, N. A. Simpson, E. G. LeBlanc, M. A. Robinson, and W. J. Geerts, *MRS Proc.* **1708** (2014).
- ¹⁰ Y. Wensheng, W. Weng, G. Zhang, Z. Sun, Q. Liu, Z. Pan, Y. Guo, P. Xu, S. Wei, Y. Zhang, and S. Yan, *Appl. Phys. Lett.* **92**, 052508 (2008).
- ¹¹ A. Bielanski, J. Deren, J. Haber, and J. Slocynski, *Trans. Faraday Soc.* **58**, 166 (1962).
- ¹² E. L. Miller and R. E. Roceleau, *J. Electrochem. Soc.* **144**, 3072 (1997).
- ¹³ J.-W. Yoon, H.-J. Kim, I.-D. Kim, and J.-H. Lee, *Nanotechnology* **24**, 444005 (2013).
- ¹⁴ S. P. Pati, B. Bhushan, A. Basumallick, S. Kumar, and D. Das, *Mater. Sci. Eng. B.* **176**, 1015 (2011).
- ¹⁵ P. Mallick, C. Rath, R. Biswal, and N. Mishra, *Indian J Phys* **83**, 517 (2009).
- ¹⁶ A. Ghosh, C. Nelson, L. Abdallah, S. Zollner, J. Vac, *Sci. Tech. A* **33**, 061203 (2015).
- ¹⁷ Y. Seo, D. Lee, and Y. Lee, *J. Korean Phys. Soc.* **55**, 129 (2009).
- ¹⁸ A. Douvalis, L. Jankovic, and T. Bakas, *J Phys: Cond. Mater.* **19**, 436203 (2007).
- ¹⁹ K. Noipa, S. Labuayai, E. Swatsitang *et al.*, *Electron. Mater. Lett.* **10**, 147 (2014).
- ²⁰ Y. Li, A. Selloni, *ACS Catal.* **4**, 1148 (2014).
- ²¹ J. Wang, J. Cai, Y. Lin, and C. Nan, *Appl. Phys. Lett.* **87**, 202501 (2005).
- ²² S. Thota, J. H. Shim, and M. S. Seehra, *J. Appl. Phys.* **114**, 214307 (2013).
- ²³ V. Raghavan, *J. Phase Equilibria Diffus.* **31**, 369 (2010).
- ²⁴ M. A. A. Talukder, Y. Cui, M. Compton, W. Geerts, L. Scolfaro, and S. Zollner, *MRS Adv. Spring* (2016).
- ²⁵ A. K. Bandyopadhyay, S. Rios, A. Tijerina, C. Gutierrez, *J. Alloy. Compd.* **369**, 217 (2004).
- ²⁶ W. Yan, W. Weng, G. Zhang *et al.*, *Appl. Phys. Lett.* **92**, 052508 (2008).
- ²⁷ G. Kresse and J. Furthmüller, *Phys. Rev. B.* **54**, 11169 (1996).
- ²⁸ P. Blöchl, *Phys. Rev. B* **50**, 17953 (1994).
- ²⁹ J. Perdew, K. Burke, and M. Ernzerhof, *Phys. Rev. Lett.* **77**, 3865 (1996).
- ³⁰ V. Anisimov, J. Zaanen, and O. Andersen, *Phys. Rev. B* **44**, 943 (1991).
- ³¹ S. Park, H. S. Ahn, C. K. Lee, H. Kim, H. Jin, H. S. Lee, S. Seo, J. Yu, and S. Han, *Phys. Rev. B* **77**, 134103 (2008).
- ³² M. Gajdoš, K. Hummer, G. Kresse, J. Furthmüller, and F. Bechstedt, *Phys. Rev. B* **73**, 045112 (2006).
- ³³ K. Rao and A. Smakula, *J. Appl. Phys.* **36**, 2031 (1965).
- ³⁴ Landolt-Börnstein, Group III Condensed Matter **41D**, 1 (2000).
- ³⁵ A. Jonscher, *J. Phys. D: Appl. Phys.* **32**, R57 (1999).